Direct *in situ* determination of the polarization dependence of physisorption on ferroelectric surfaces

DONGBO LI[1]*, MOSHA H. ZHAO[2]*, J. GARRA[1], A. M. KOLPAK[3], A. M. RAPPE[3], D. A. BONNELL[1] AND J. M. VOHS[2†]

[1]Department of Materials Science and Engineering; [2]Department of Chemical and Biomolecular Engineering; [3]The Makineni Theoretical Laboratories, Department of Chemistry, University of Pennsylvania, Philadelphia, Pennsylvania 19104, USA

*These authors contributed equally to this work

†e-mail: vohs@seas.upenn.edu

Published online: 11 May 2008; doi:10.1038/nmat2198

The ability to manipulate dipole orientation in ferroelectric oxides holds promise as a method to tailor surface reactivity for specific applications. As ferroelectric domains can be patterned at the nanoscale[1], domain-specific surface chemistries may provide a method for fabrication of nanoscale devices. Although studies over the past 50 yr have suggested that ferroelectric domain orientation may affect the energetics of adsorption, definitive evidence is still lacking[2–5]. Domain-dependent sticking coefficients are observed using temperature-programmed desorption and scanning surface potential microscopy, supported by first-principles calculations of the reaction coordinate. The first unambiguous observations of differences in the energetics of physisorption on ferroelectric domains are presented here for CH_3OH and CO_2 on $BaTiO_3$ and $Pb(Ti_{0.52}Zr_{0.48})O_3$ surfaces.

Ferroelectric perovskites have a spontaneous electric polarization with multiple possible orientations relative to the crystallographic axes. This behaviour is used in the electronic ceramics industry, and in high-density information storage[1]. Although electron-exchange reactions at liquid–ferroelectric–solid interfaces are known to be domain orientation specific[6–8], attempts to quantify the effect of domain orientation on adsorption from the gas phase have been largely inconclusive[2–5]. This is due in part to the fact that most previous studies have characterized adsorption on powders of ferroelectric compounds, where domain orientation could not be systematically controlled. A recent study by Yun *et al.*[9], however, provides compelling evidence for ferroelectric-domain-orientation-dependent adsorption, where a difference in the interaction of 2-propanol with separately poled c^+ and c^- oriented $LiNbO_3(0001)$ surfaces was observed. Here, we have demonstrated polarization dependencies for reactive sticking coefficients on $BaTiO_3$ and $Pb(Ti_{0.52}Zr_{0.48})O_3$ (PZT). Samples were poled *in situ* to ensure that the polarization direction was the only parameter varied and multiple methods were used to characterize adsorption. The experimental results are compared with first-principles calculations and together these show a polarization-dependent, physisorption energy well. This work constitutes the first definitive observation of domain dependencies for sticking coefficients on ferroelectric surfaces.

$BaTiO_3$ consists of corner-linked oxygen octahedra containing Ti^{4+}, with Ba^{2+} in the interstices between the octahedra, Fig. 1a. Distortions in the octahedra result in multiple ferroelectric phases. In the cubic-to-tetragonal transition ($T_C = 120\,^{\circ}C$), Ti^{4+} moves towards the oxygen apices creating electric dipoles that align in a parallel fashion to produce domains. The c^+, c^- and a domains have polarization parallel, antiparallel and perpendicular to the surface normal, respectively. PZT has a distorted perovskite structure with Ti^{4+} and Zr^{4+} ions randomly occupying octahedral sites with polarization directed along the unit-cell diagonal. $BaTiO_3(001)$ single crystals and $BaTiO_3$ and PZT thin films were used in this study. The $BaTiO_3(001)$ surface was atomically smooth and terminated with c^+, c^- and a domains, Fig. 1b,c. The $BaTiO_3$ thin films were polycrystalline with 70–200 nm grains and roughness <10 nm, Fig. 1d. Temperature-programmed desorption (TPD) of CH_3OH was used to probe surface–adsorbate interactions for the $BaTiO_3$ thin film, whereas scanning surface potential microscopy (SSPM) and CO_2 adsorption were used for the $BaTiO_3(001)$ and PZT thin film. Ferroelectric domains were oriented *in situ* using planar electrodes or a conductive atomic force microscope (AFM) tip, and all experiments were conducted in ultrahigh vacuum (UHV).

The amount of CH_3OH that desorbs from $BaTiO_3$ after a constant subsaturation exposure (Fig. 2) is strongly and reproducibly polarization dependent. Before dosing, blank TPD runs up to 700 K were featureless, demonstrating that adsorption from the chamber background (for example, H_2 or H_2O) did not contribute to the TPD results. After dosing, CH_3OH (methanol) desorbs at 365 K with a high-temperature (T) tail that contains a further small methanol peak at 580 K. Other desorbing species were water (not shown) and formaldehyde, at 590 K. The saturation coverage of chemisorbed species was low and estimated to be <0.20 ML. This behaviour is similar to that observed for CH_3OH on TiO_2 (refs 10–12) and other oxide surfaces[13,14] and is consistent with CH_3OH adsorbing dissociatively on defect sites to produce adsorbed methoxide species that either desorb recombinatively or react to produce formaldehyde[10–14]. The primary effect of polarization orientation is on the amount of CH_3OH adsorbed, which increases in the following order: $c^+ <$ unpoled $< c^-$. The

© 2008 Nature Publishing Group

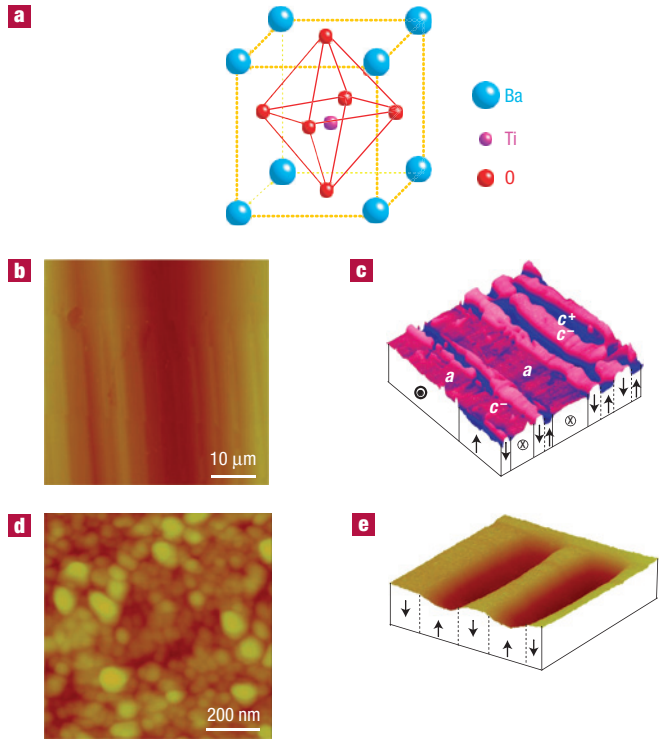

Figure 1 Surface and domain structure of $BaTiO_3$ samples. **a**, Crystallographic structure of $BaTiO_3$. **b**, Topography of single-crystal $BaTiO_3$(001) measured by AFM. Atomically smooth facets are superimposed on domains. **c**, Domain structure on the same surface of $BaTiO_3$(001) imaged by SSPM. **d**, Topography of polycrystalline $BaTiO_3$ thin film measured by AFM. **e**, SSPM of oppositely poled regions on the $BaTiO_3$ film.

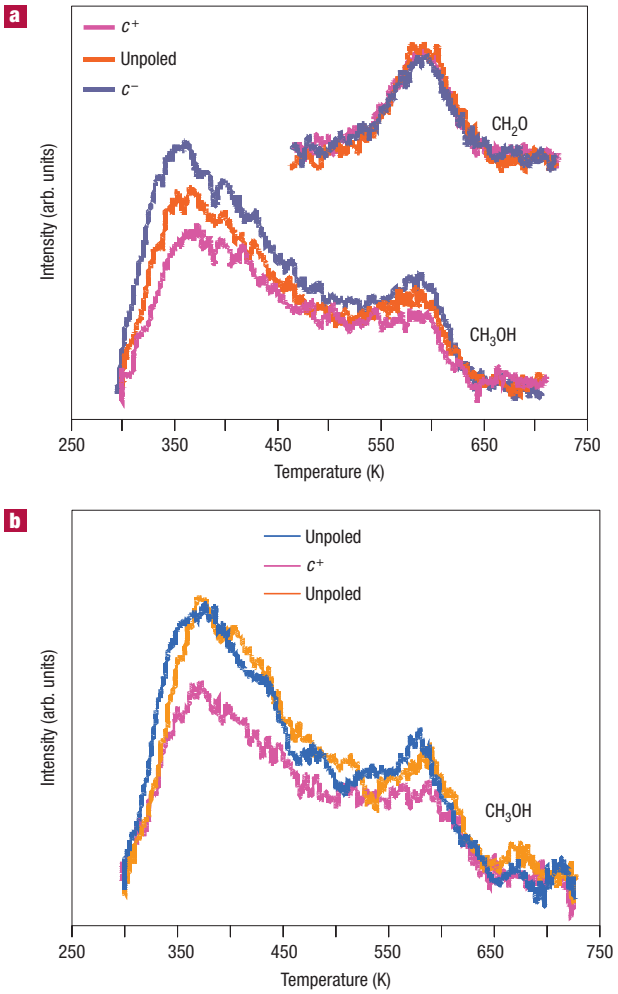

Figure 2 TPD spectra obtained following exposure of the $BaTiO_3$ thin film to a subsaturation 20 L dose of CH_3OH as a function of ferroelectric polarization. **a**, The CH_3OH and CH_2O desorption signals for a series of runs where the polarization was in the following order: c^+, unpoled, c^-. **b**, The CH_3OH signal for a series where the polarization was in the following order: unpoled, c^+, unpoled.

unpoled surface contains regions of both positive and negative polarity and is expected to be intermediate between that of c^+ and c^-, as observed experimentally. In Fig. 2b, the polarization sequence is reversed to demonstrate reproducibility. Whereas the amount of CH_3OH that adsorbs is a function of ferroelectric polarization, the shape of the desorption curves is not. Thus, whereas the similar TPD shape suggests that chemisorption energy is nearly polarization independent for CH_3OH on $BaTiO_3$, the change in TPD integrated area demonstrates that the reactive sticking coefficient S (the fraction of the impinging molecules that ultimately react to form a chemisorbed species) and the physisorption energy (as discussed below) strongly depend on substrate polarization.

Concurrently, AFM and SSPM were combined to study the adsorption of CO_2 onto $BaTiO_3$(001) and the PZT thin film. Before CO_2 exposure, an AFM tip was used to pole c^+ and c^- domains in close proximity (Fig. 3a,e). For nearly stoichiometric $BaTiO_3$(001), the surface potential was invariant with CO_2 exposure up to 500 L (langmuirs) and TPD data also showed that CO_2 did not adsorb, so the $BaTiO_3$(001) was slightly reduced by vacuum annealing. This resulted in surface potential changes on CO_2 exposure (Fig. 3b,f), indicating that chemisorption is defect mediated, which is common for oxides. After various CO_2 doses, the surface potentials of $BaTiO_3$(001) and the PZT thin film were measured (Fig. 3c,g).

For both $BaTiO_3$(001) and the PZT thin film, the magnitude of the average surface potentials of both the c^+ and c^- domains decreases monotonically with CO_2 dose. The surface potential initially changes linearly with dose, and then more slowly as saturation coverage is approached. As defects are created at high temperature and experiments are then carried out at room temperature, poling *in situ* is not likely to affect the concentration of defect sites, and therefore the saturation coverage of CO_2 on the c^+ and c^- domains is nearly equal. Thus, the trends observed in Fig. 3c,g can be attributed to differences in both the CO_2 coverage at constant exposure and the magnitude of the effect of adsorbed CO_2 on the surface potential on the two polarizations. Because the chemisorption is defect mediated, the saturation coverage is low and neighbouring adsorbates do not interact, so the surface potential change is linearly proportional to coverage. The coverage θ is the fraction of sites per area, N_0, that are occupied, $N = \theta N_0$. The reactive sticking coefficient S is the fraction of impinging molecules that eventually become chemisorbed. For an ideal gas with dose L, the number of molecules that impinge is $L/\sqrt{2\pi m k_B T}$. We therefore plot

$$\frac{\theta(L)}{\theta_{max}} = \frac{V(L) - V(0)}{V_{max} - V(0)} = \frac{SL}{\theta_{max} N_0 \sqrt{2\pi m k_B T}} \quad (1)$$

© 2008 Nature Publishing Group

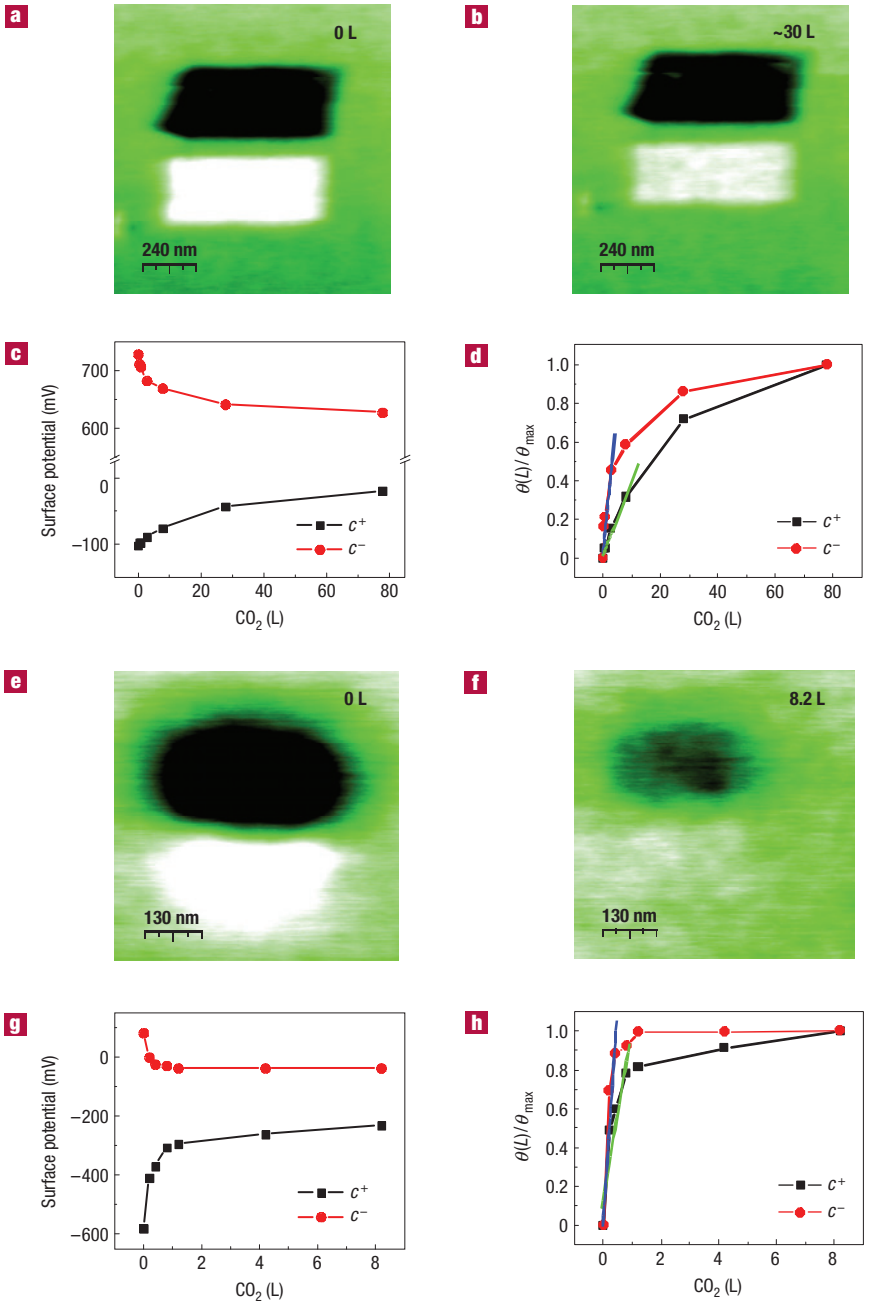

Figure 3 Influence of CO_2 adsorption on the surface potential of $BaTiO_3$(001) and a PZT thin film. a, Surface potential maps of c^+ and c^- domains (700 nm × 700 nm) on $BaTiO_3$(001), which were poled by an external electrical field applied by a conductive AFM tip scanning over the surface. Ferroelectric domains were poled positively (negatively) in the dark (bright) area and showed negative (positive) surface potential due to the opposite compensating charges. The areas surrounding c^+ and c^- domains represent in-plane *a* domains. **b**, Surface potential maps after exposure to 30 L of CO_2. **c**, Average surface potential versus CO_2 dose on $BaTiO_3$(001). **d**, $\theta(L)/\theta_{max}$, (see equation (1)) versus CO_2 dose. *S* is proportional to the slope of the line. **e–h**, Corresponding data for CO_2 adsorption on the polycrystalline PZT thin film.

in Fig. 3d,h. The dose dependencies of the potential are linear for a significant range, with slopes for c^+ and c^- that differ by factors of 3.7 and 2.5 for $BaTiO_3$ and PZT, respectively, showing that the reactive sticking coefficient is polarization dependent and constant for a significant range of θ and L. As discussed below, this is strong evidence that S reflects the physisorption energy well.

Chemisorption (Fig. 4a,b) occurs either by direct collisional activation, where the molecule forms chemical bonds with the surface during impact[15], or precursor-mediated adsorption, where the molecule is first trapped into a weakly bound physisorbed state that is a precursor for reaction to the chemisorbed state[16–18]. Our results show that adsorption is precursor mediated for all systems studied. The TPD data for CH_3OH show that S is strongly affected by ferroelectric polarization, but the chemisorption energy is not. This means that the increased S is due to a greater physisorption energy, leading to a longer residence time for the precursor state and

© 2008 Nature Publishing Group

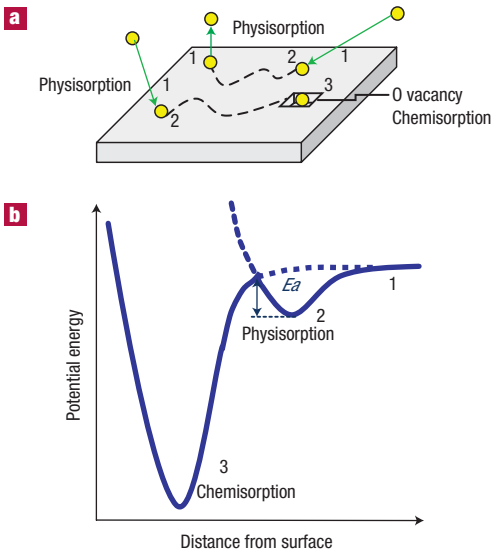

Figure 4 Precursor-mediated molecular adsorption on defective ferroelectric oxide surfaces. a, The gas-phase molecule physisorbs to the oxide surface, where it diffuses until reaching and chemisorbing at an O vacancy, or eventually desorbing. **b**, Schematic diagram of the potential energy as a function of the distance from the surface.

a greater chance of finding a chemisorption defect site. The SSPM data for CO_2 show that S is constant, leading to a linear rise of θ versus L. If S were influenced by chemisorption, S would decrease continually as θ rises, making fewer chemisorption sites available. The linearity of θ versus L demonstrates that S is controlled by the rate at which molecules enter a physisorption precursor state.

The following mechanism is therefore proposed for molecular adsorption onto ferroelectric oxides. Impinging gas-phase molecules become trapped into a shallow physisorption well, dominated by van der Waals interactions and influenced by polarization. These interactions are not site specific, and the trapped precursor can move along the surface. Many trapped molecules spend a short time on the surface and then desorb; however, if one encounters an active site (for example, an oxygen vacancy), the precursor may react to form a chemisorbed species, in which chemical bonds are formed. Formation of the chemisorbed species may require sufficient energy to overcome an activation barrier.

The precursor-mediated adsorption model enables us to quantify the change in the physisorption well due to polarization. As mentioned above, Fig. 3d gives the ratio of S for the two polarizations on $BaTiO_3(001)$, $S_{c-}/S_{c+} = 3.7$, which is the ratio of kinetic rates of physisorption onto the two surfaces. Assuming Arrhenius kinetics with a late transition state[19,20], the difference in physisorption energy on the c^- and c^+ domains is estimated to be $3.4\,kJ\,mol^{-1}$. A similar analysis for PZT gives an estimated difference of $2.4\,kJ\,mol^{-1}$. As physisorption energies for small molecules are typically 10–20 $kJ\,mol^{-1}$, the 2.4–3.4 $kJ\,mol^{-1}$ difference due to polarization is consistent with a change in the depth of the physisorption well. From a molecular perspective, several mechanisms could account for the dependence of the physisorption energy on ferroelectric polarization, including changes in dipole–dipole interactions between the adsorbate and the surface and differences in the surface structure of c^- and c^+ regions.

Having experimentally demonstrated the polarization dependence of physisorption energies, we now discuss an atomistic interpretation of the chemisorption processes for CO_2, incorporating density functional theory (DFT) calculations. As discussed above, vacuum annealing enabled chemisorption of CO_2, so we propose that chemisorption at oxygen vacancies predominates. DFT calculations were used to study this process. Adsorption energies were calculated for CO_2 on both c^+ and c^- TiO_2-terminated $BaTiO_3(001)$ surfaces containing 1/3 of a monolayer of oxygen vacancies. For the c^+ surface, the DFT results show that dissociative adsorption of CO_2 at an oxygen vacancy producing CO adsorbed on a neighbouring Ti cation is the energetically preferred pathway. Oxygen vacancies on the c^- surface help compensate the polarization charge and dissociative adsorption of CO_2, resulting in filling of the vacancy being less energetically favourable. Consequently, on this surface, molecular adsorption of CO_2 at defect sites is the most energetically favourable mode of adsorption. The calculations also show that this difference, associative versus dissociative adsorption, explains why the magnitudes and directions of the changes in the surface potential with CO_2 adsorption are different on the c^+ and c^- surfaces.

These results represent the first direct observation of the effect of ferroelectric polarization on physisorption energies using identical surfaces that were poled *in situ*. TPD and SSPM demonstrate how oxide polarization affects the reactive sticking coefficient S for a range of temperature T and dose L, as a direct consequence of the physisorption energy well. DFT results show that the mode of CO_2 chemisorption is polarization dependent. The effect of polarization on physisorption energies was found to be general in that it occurs for adsorption of CH_3OH and CO_2, on $BaTiO_3$ and PZT.

METHODS

A 150-nm-thick $BaTiO_3$ film was grown on a conductive $TiO_2(110)$ substrate using a sol–gel method similar to that described by Schwartz *et al.*[21] X-ray diffraction confirmed that the film consisted of single-phase, randomly oriented grains. Polycrystalline PZT thin films ~16 nm thick were prepared by a similar sol–gel process on $SrTiO_3$/Si substrates. X-ray diffraction confirmed that the PZT grains exhibited (100) crystallographic orientation. A $BaTiO_3(001)$ single crystal (5 mm × 5 mm × 1 mm) was obtained from Superconductive Components. To facilitate poling, the single crystal was mechanically thinned to 100 μm from the back, leaving the polished surface with roughness less than 0.25 nm.

For the TPD studies, the $BaTiO_3$ film was annealed at 973 K in air to remove surface impurities and then annealed at 600 K after being placed in the UHV chamber. This sample was macroscopically poled in UHV by bringing it into contact with a polished copper electrode and applying a ±4 V bias while the sample was heated to 450 K, approximately 60 K above T_c. The field was maintained during cooling to room temperature. For the SSPM studies, $BaTiO_3(001)$ and PZT thin-film samples were annealed at ~500 K for 20 min after being introduced into the UHV chamber to remove surface adsorbates. After that, small regions of the surface were poled using an AFM (Omicron VT-AFM/STM) with a conductive tip. The tip was contacted to the surface and a bias of ±2 V was applied while it was rastered over the surface. For $BaTiO_3(001)$, the tip was scanned over the surface at 1.67 Hz, reorienting the domains perpendicular to the crystal surface plane. Reversing the sign of the applied bias during a scan resulted in adjacent oppositely oriented domains. For the PZT thin film, a bias of ±1 V was applied to the tip during domain switching.

TPD experiments were conducted in a UHV surface analysis system equipped with a mass spectrometer (UTI) for measuring gas partial pressures. During TPD, the $BaTiO_3/TiO_2(110)$ was heated at $2\,K\,s^{-1}$ and the temperature was measured with a type-K thermocouple attached to the edge of the sample using a ceramic adhesive. Methanol was admitted into the UHV system using a variable leak valve.

SSPM (also called Kelvin probe microscopy) was used to map the surface potential as a function of gas exposure. SSPM is a non-contact

© 2008 Nature Publishing Group

technique that provides a direct measure of local variations in surface potential on the nanometre scale. During SSPM, an oscillating electric signal, $V = V_{\mathrm{d.c.}} + V_{\mathrm{a.c.}} \sin(\omega t)$, is applied to the conductive cantilever/tip. The first harmonic of the force between the tip and the surface is given by:

$$F_{1\omega}(z) = \frac{\partial C(z)}{\partial (z)} (V_{\mathrm{d.c.}} - V_S) V_{\mathrm{a.c.}}$$

where $C(z)$ is the tip–surface capacitance, which is dependent on tip geometry, surface topography and tip–surface separation, z. When a d.c. bias on the tip matches the surface potential, the force goes to zero. A map of this nullifying bias yields the spatial variation in surface potential. On ferroelectric surfaces, the measured potential is a convolution of the ferroelectric polarization and compensation charge resulting from mobile carriers in the crystal and adsorption on the crystal[22,23].

DFT calculations were carried out within the generalized gradient approximation and ultrasoft pseudopotentials using the dacapo code, with a 30 Ryd cutoff energy and a $4 \times 4 \times 1$ Monkhorst–Pack k-point grid. The systems were composed of six layers of $BaTiO_3$ capped on one end by three layers of Pt metal to accurately simulate the surface of a thick film at lower computational cost. Here, a layer is defined as a BaO or TiO_2 plane in the (001) direction. The atoms in the bottom four layers were fixed in the theoretical bulk ferroelectric positions, with the polarization perpendicular to the surface. The top two layers and adsorbates were relaxed completely until the forces on each atom were below 1 meV nm^{-1}. A dipole correction was included in the centre of the $\approx$1.2 nm vacuum separating the film from its periodic image. In all cases, the surface consisted of a TiO_2 plane, consistent with recent experimental and theoretical predictions of the $BaTiO_3$ surface structure, and the in-plane lattice constant of theoretical bulk $BaTiO_3$, $a = 0.399$ nm, was used to model unstrained films.

Received 13 December 2007; accepted 16 April 2008; published 11 May 2008.

References

1. Scott, J. F. Applications of modern ferroelectrics. *Science* **315**, 954–959 (2007).
2. Parravano, G. Ferroelectric transitions and heterogenous catalysis. *J. Chem. Phys.* **20**, 342–343 (1952).
3. Cabrera, A. L. *et al.* Catalysis of reactions involving oxides of carbon and nitrogen by the ferroelectric compound potassium niobate. *Mater. Res. Bull.* **14**, 1155–1166 (1979).
4. Cabrera, A. L., Tarrach, G., Lagos, P. & Cabrera, G. B. Influence of crystallographic phase transitions in small ferroelectric particles on carbon dioxide adsorption. *Ferroelectrics* **281**, 53–66 (2002).
5. Cabrera, A. L., Vargas, F., Zarate, R. A., Cabrera, G. B. & Espinosa-Gangas, J. The size dependent adsorption properties of ferroelectric particles. *J. Phys. Chem. Solids* **62**, 927–932 (2001).
6. Kalinin, S. V. *et al.* Ferroelectric lithography of multicomponent nanostructures. *Adv. Mater.* **16**, 795–799 (2004).
7. Giocondi, J. L. & Rohrer, G. S. Spatially selective photochemical reduction of silver on the surface of ferroelectric barium titanate. *Chem. Mater.* **13**, 241–242 (2001).
8. Giocondi, J. L. & Rohrer, G. S. Structure sensitivity of photochemical oxidation and reduction reactions on $SrTiO_3$ surfaces. *J. Am. Ceram. Soc.* **86**, 1182–1189 (2003).
9. Yun, Y., Kampschulte, L., Li, M., Liao, D. & Altman, E. I. Effect of ferroelectric poling on the adsorption of 2-propanol on $LiNbO_3$(0001). *J. Phys. Chem. C* **111**, 13951–13956 (2007).
10. Henderson, M. A., Otero-Tapia, S. & Castro, M. E. The chemistry of methanol on the surface: the TiO_2 (110) influence of vacancies and coadsorbed species. *Faraday Discuss.* **114**, 313–329 (1999).
11. Kim, K. S. & Barteau, M. A. Reactions of methanol on TiO_2(001) single crystal surfaces. *Surf. Sci.* **223**, 13–32 (1989).
12. Farfan-Arribas, E. & Madix, R. J. Different binding sites for methanol dehydrogenation and deoxygenation on stoichiometric and defective TiO_2(110) surfaces. *Surf. Sci.* **544**, 241–260 (2003).
13. Ferrizz, R. M., Wong, G. S., Egami, T. & Vohs, J. M. Structure sensitivity of the reaction of methanol on ceria. *Langmuir* **17**, 2464–2470 (2001).
14. Dilara, P. A. & Vohs, J. M. Structure sensitivity in the reaction of methanol on ZrO_2. *Surf. Sci.* **321**, 8–18 (1994).
15. Lohokare, S. P., Crane, E. L., Dubois, L. H. & Nuzzo, R. G. Collision-induced activation of the beta-hydride elimination reaction of isobutyl iodide dissociatively chemisorbed on Al(111). *J. Chem. Phys.* **108**, 8640–8650 (1998).
16. Brown, D. E., Moffatt, D. J. & Wolkow, R. A. Isolation of an intrinsic precursor to molecular chemisorption. *Science* **279**, 542–544 (1998).
17. Carlsson, A. F. & Madix, R. J. Intrinsic and extrinsic precursors to adsorption: Coverage and temperature dependence of Kr adsorption on Pt(111). *J. Chem. Phys.* **114**, 5304–5312 (2001).
18. Kisliuk, P. The sticking probabilities of gases chemisorbed on the surfaces of solids. *J. Phys. Chem. Solids* **3**, 95–101 (1957).
19. Bronsted, J. N. Acid and basic catalysis. *Chem. Rev.* **5**, 231–338 (1928).
20. Evans, M. G. & Polanyi, M. Inertia and driving force of chemical reactions. *Trans. Faraday Soc.* **34**, 11–24 (1938).
21. Schwartz, R. W. *et al.* Control of microstructure and orientation in solution-deposited $BaTiO_3$ and $SrTiO_3$ thin films. *J. Am. Ceram. Soc.* **82**, 2359–2367 (1999).
22. Kalinin, S. V. & Bonnell, D. A. Local potential and polarization screening on ferroelectric surfaces. *Phys. Rev. B* **63**, 125411 (2001).
23. Kalinin, S. V., Johnson, C. Y. & Bonnell, D. A. Domain polarity and temperature induced potential inversion on the $BaTiO_3$(100) surface. *J. Appl. Phys.* **91**, 3816–3823 (2002).

Acknowledgements

We gratefully acknowledge support of this work by the NSF MRSEC program (grant no. DMR05-20020). A.M.K. and A.M.R. also acknowledge support from the US Air Force Office of Scientific Research (grant no. FA9550-07-1-0397) and the US Department of Energy, Division of Basic Energy Sciences (grant no. DE-FG02-07ER15920) and computational support from the HPCMO of the US DoD.

Author information

Reprints and permission information is available online at http://npg.nature.com/reprintsandpermissions. Correspondence and requests for materials should be addressed to J.M.V.

© 2008 Nature Publishing Group